Atomtronics: Ultracold-atom analogs of electronic devices

B. T. Seaman, M. Krämer, D. Z. Anderson, and M. J. Holland
JILA, National Institute of Standards and Technology and Department of Physics, University of Colorado, Boulder, Colorado 80309-0440, USA
(Received 23 June 2006; published 20 February 2007)

Atomtronics focuses on atom analogs of electronic materials, devices, and circuits. A strongly interacting ultracold Bose gas in a lattice potential is analogous to electrons in solid-state crystalline media. As a consequence of the gapped many-body energy spectrum, cold atoms in a lattice exhibit insulatorlike or conductorlike properties. *P*-type and *N*-type material analogs are created by introducing impurity sites into the lattice. Current through an atomtronic wire is generated by connecting the wire to an atomtronic battery which maintains the two contacts at different chemical potentials. The design of an atomtronic diode with a strongly asymmetric current-voltage curve exploits the existence of superfluid and insulating regimes in the phase diagram. The atom analog of a bipolar junction transistor exhibits large negative gain. Our results provide the building blocks for more advanced atomtronic devices and circuits such as amplifiers, oscillators, and fundamental logic gates.

DOI: 10.1103/PhysRevA.75.023615 PACS number(s): 03.75.Kk, 05.30.Jp, 03.75.Lm, 73.43.Nq

I. INTRODUCTION

A collection of ultracold atoms subject to a spatially periodic potential can exhibit behavior analogous to electrons in a crystal lattice. This fact has been established in an impressive series of experiments with Bose-Einstein condensates and Fermi gases in optical lattices produced by interfering laser beams [1–10]. The analogy between ultracold atoms in lattice potentials and electrons in crystals is manifestly a rich one. It extends to strongly interacting ultracold Bose gases which exhibit both superfluid and insulating behavior, and feature a gapped many-body energy spectrum. The tunability of interactions in optical lattices has led to the spectacular demonstration of these properties [11–13]. In this work we introduce analogs of electronic materials, including metals, insulators, and semiconductors, in the context of ultracold strongly interacting bosons. We use lattice defects to achieve behavior similar to doped *P*-type and *N*-type semiconductors. The interest is to adjoin *P*-type and *N*-type lattices to create diodes and then *NPN* or *PNP* structures to achieve behavior similar to that of bipolar junction transistors. We show that such heterogeneous structures can indeed be made to mimic their electronic counterparts. Ruschhaupt and Muga [14] have described an atom device with diodelike behavior, and Micheli *et al.* [15] have proposed a single-atom transistor that serves as a switch (see also Refs. [16–20]). Both of these devices depend on control and coherence at the single atom level. Moreover, Stickney *et al.* [21] have recently demonstrated that a Bose-Einstein condensate in a triple well potential can exhibit behavior similar to that of a field effect transistor. Our intent is to establish ultracold atom analogs of electronic materials and semiconductor devices that can be used to leverage the vast body of electronic knowledge and heuristic methods. From semiconductor materials and fundamental devices, the analogy expands into what can be referred to as *atomtronics*. With diodes and transistors in hand, it is straightforward to conceive of atom amplifiers, oscillators, flip-flops, logic gates, and a host of other atomtronic circuit analogs to electronic circuits. Such a set of devices can serve as a toolbox for implementing and managing integrated circuits containing atom optical elements [22–24] or quantum computation components [25–27] and might be of particular interest in the context of rapidly advancing atom chip technologies [28,29].

Atoms in periodic structures and electrons in solid state crystals have much in common. In both systems, particle motion occurs by tunneling through the potential barrier separating two lattice sites. A particle, an electron or an atom, can delocalize over the entire lattice and sustain currents. In both systems, currents are created when there is a potential gradient which causes the particles to move from a region of higher potential to a region of lower potential. In electronics, potentials arise from electric fields. In atomtronics, potential gradients can be understood in terms of chemical potential gradients. The characteristics of both electronic and atomtronic devices are examined by using a battery to apply a potential difference across the system and observing the response in the current.

Different types of electronic conductors exist because electrons in a crystal structure occupy states of an energy spectrum that features a band structure. The materials can carry a current, i.e., are conducting, only if the highest occupied energy band is only partially filled with electrons. On the other hand, the system is an insulator if all occupied bands are full. These properties of electronic materials can be directly reproduced with weakly interacting fermionic atoms in periodic potentials.

Using fermionic atoms is not the only way in which analogs of electronic materials can be created. In this paper, we focus on ultracold strongly interacting bosonic atoms in periodic structures. These systems can also be made to behave similarly to their electronic counterparts. Strong repulsive interactions prevent atoms from occupying the same lattice site, mimicking the fermionic behavior of electrons. Hence, a current can flow easily as long as there are empty sites available. However, once the filling reaches one atom per site, the system becomes an insulator. A large energy gap given by the repulsive onsite interaction must be overcome in order to add another particle to this configuration. Particles added in ex-

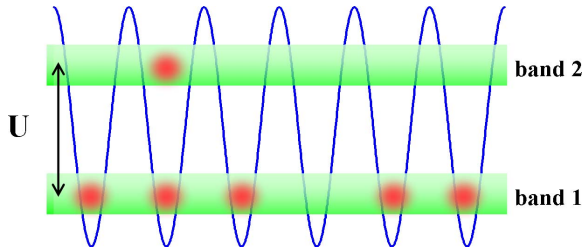

FIG. 1. (Color online) Schematic of the atomtronic many-body energy band structure of strongly interacting bosons in a lattice. The first band is made up of all states with a filling of less than one atom per site while the second band contains all states with filling between one and two atoms per site. The two bands are separated by the onsite repulsive interaction U.

cess of a filling of one atom per site can again carry a current since they can move around freely above the filled layer of one atom per site. The system remains a conductor until it arrives at a filling of two atoms per site and becomes an insulator again.

These properties show that a strongly interacting Bose gas features a close analog of the band structure of electronic materials. The filling of the bands determines whether a material is a conductor or an insulator. There is, however, an important difference between atomtronic and electronic systems with respect to the band structure. The band structure of strongly interacting bosons does not describe states that can be occupied by a single particle independently of the configuration of others, but represents the energies of many-body states. While the energy gap is due to the Pauli exclusion principle combined with the single-particle band structure in the case of electrons, the gap arises from the onsite repulsive interaction between atoms in the bosonic case. In this paper, we will speak of *many-body* energy bands in the case of bosonic systems to take account of this important difference. The many-body band structure of strongly interacting bosons in a lattice is depicted schematically in Fig. 1. The lowest band is made up of states with between zero and one atom per site. The next band contains all states with one to two atoms per site. Higher bands are formed analogously. The highest occupied band of a conductor is only partially filled while insulators are characterized by full bands.

Apart from the many-body character of the band structure, a second important feature of the atomtronic system is that the atomtronic conductor exhibits superfluid rather than normal flow and in that aspect resembles an electronic superconductor.

In this paper, the behavior of atomtronic materials in simple circuits is presented and we show how to use these materials to build more complex circuit devices, specifically diodes and bipolar junction transistors. The paper is structured as follows. Section II introduces the Bose-Hubbard formalism that will be used to describe the atomtronic systems. In particular, it discusses the zero temperature phase diagram and the properties of an atomtronic battery. Doped atomtronic materials and the current-voltage behavior of atomtronic wires will be discussed in Sec. III. A diode obtained by combining a *P*-type and an *N*-type atomtronic material with a voltage bias applied by a battery is examined in Sec. IV. Section V presents the atomic analog of a semiconductor bipolar junction transistor. Finally, Sec. VI contains remarks on possible applications, on the differences between atomtronic devices and their electronic counterparts and on future perspectives. The appendix contains details of the calculation methods that were used throughout the paper.

II. BOSE-HUBBARD FORMALISM

The zero temperature quantum phases of bosons in a lattice are key to understanding the different kinds of atomtronic materials. A system of repulsive bosons in a one-dimensional chain of lattice sites can be modeled with the Bose-Hubbard Hamiltonian

$$\hat{H} = \frac{U}{2}\sum_i \hat{n}_i(\hat{n}_i - 1) - J\sum_{\langle ij\rangle} \hat{a}_i^\dagger \hat{a}_j + \sum_i (\epsilon_i - \mu)\hat{n}_i, \qquad (1)$$

where $\hat{a}_i$ is the annihilation operator for a particle at site i, $\hat{n}_i \equiv \hat{a}_i^\dagger \hat{a}_i$ is the number operator at site i, U is the onsite repulsive interaction strength, J is the hopping matrix element between nearest neighbors, $\langle ij\rangle$ labels nearest neighbors, ϵ_i is the external potential at site i and μ is the chemical potential of the system. The Bose-Hubbard Hamiltonian is obtained by retaining only the contributions of the lowest single particle Bloch band to the Hilbert space and by making a tight binding approximation (for a review see Ref. [30]) and yields an accurate description of an ultracold dilute Bose gas in a periodic potential at low energies. The zero temperature phase diagram of this Hamiltonian was first studied by Fisher *et al.* [31].

For very large onsite repulsion, $U \gg J$, the system enters the regime of *fermionization* where bosons are impenetrable and only two Fock states, $|n_i\rangle$ and $|n_i+1\rangle$, are needed at each site to accurately describe the system (two-state approximation). Note that this is equivalent to mapping bosonic operators onto fermionic ones via the Jordan-Wigner transformation [32,33]. The data presented in this paper is obtained by considering the system described by the Hamiltonian, Eq. (1), in the fermionized regime. We have verified that the error resulting from the two-state approximation becomes negligible for $U \geqslant 100J$ (see also Ref. [34]).

A. Phase diagram

The phase diagram of the Bose-Hubbard Hamiltonian contains information about the many-body band structure of the system. At zero temperature, the Bose-Hubbard model has two distinct phases, a Mott-insulating phase and a superfluid phase. Figure 2 presents the boundary between the conducting and insulating phases as a function of the hopping parameter J/U and the chemical potential μ/U. The Mott-insulating phase is entered below a critical value of J/U for an integer number of particles per site. In this phase, strong interactions completely block particle motion rendering the gas incompressible, that is $\partial n/\partial \mu = 0$, where n is the average filling of a site. The two lobes shown limit the Mott-insulator zones with one atom per site (lower lobe, MI1) and two atoms per site (upper lobe, MI2). The remainder of the de-

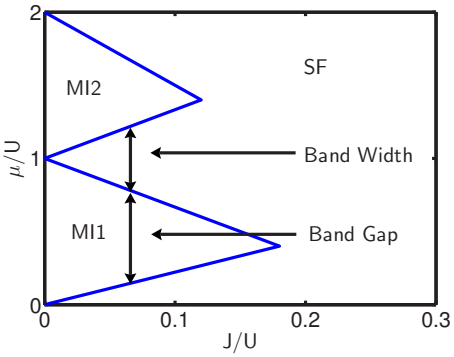

FIG. 2. (Color online) Zero temperature phase diagram of a Bose gas obtained from Eq. (2) for an infinite one-dimensional lattice using the two-state approximation (fermionized regime, $U \gg J$). At large values of J/U the gas is superfluid (SF). Below a critical value of J/U the system enters a Mott-insulator phase (MI) for integer filling, while it remains superfluid for noninteger filling. The MI1 Mott-insulator region has one atom per site and the MI2 region has two atoms per site. The width of a Mott lobe at a given J/U gives the size of the band gap in the many-body band structure while the width of a band is given by the width of the superfluid region. The Mott lobe boundaries are linear due to the use of the two-state approximation [35].

picted part of the phase diagram is in the conducting superfluid phase, labeled SF. The superfluid phase is obtained for noninteger filling. No insulating phase exists for values of J/U larger than ~ 1. Note that the triangular, nonrounded, shape of the Mott lobes in Fig. 2 is due to the two-state approximation becoming increasingly inaccurate as J/U is increased [35].

Each value of μ/U and J/U maps onto a particular lattice filling, n. Figure 2 is obtained from the relation between these parameters in the superfluid phase for an infinite number of lattices sites and strong interactions ($J \ll U$) [36]

$$\mu = U(m-1) + (-1)^m 2mJ\cos(\pi n), \tag{2}$$

where $m=1,2,\ldots$ is the band index and the filling n satisfies $(m-1) \leqslant n \leqslant m$. The superfluid-insulator phase boundaries presented in Fig. 2 are obtained by setting n to an integer and $m=n$ for the lower boundary and $m=n+1$ for the upper boundary. The expression Eq. (2) is derived using a Jordan-Wigner transformation approach within the two-state approximation.

Plotting the phase diagram as a function of μ/U rather than the number of particles is useful because in this way the gaps between many-body bands become visible. The size of the gaps are given by the widths of the insulating zones, whereas the sizes of the bands are given by the widths of the superfluid zones. Note that the size of the gaps depend on the value of J/U. In order to have access to both insulating and conducting phases, the ratio J/U must be small. If this ratio is too large there is no well defined gap and therefore no transition to an insulating phase for integer filling. The basic ideas presented in this paper rely on this condition being satisfied. They do not require the stronger condition $U \gg J$ for fermionization. The condition of fermionization is assumed merely to facilitate calculations.

B. Atomtronic battery

Just as for electronic circuits, the atomtronic version of a battery is crucial but it is also subtle. In this section, we identify the basic properties and actions of the atom analog of a battery.

Energy for electronic circuits is supplied by sources of electric potential. Furthermore, electric potentials are used to set the bias points of circuit elements to achieve their desired behavior. For simplicity, we will use the term battery to refer to a device that provides a fixed potential difference and can supply an electric current or atomic flux.

In the electronic case, one is interested in the electric potential difference, or the voltage, between two points. A specific potential difference between two points within a device or circuit is achieved by connecting those two points to the terminals of a battery. In an atomtronic circuit, the function of the battery is to hold the two contacts at different values of the chemical potential, say μ_L on the left and μ_R on the right. The applied voltage is then defined by

$$V \equiv \mu_L - \mu_R. \tag{3}$$

The current flows from higher to lower chemical potential. Chemical potential difference in atomtronic systems is analogous to electric potential difference in electronic systems. Note that the equilibrium value of the chemical potential is important since it sets the average filling of the lattice.

To understand the physics underlying this concept, note that bringing the system with chemical potential μ in contact with a battery pole of chemical potential $\mu_L > \mu$ leads to the injection of Δn particles. The magnitude of Δn is given by the difference in filling of states with chemical potentials μ and μ_L and can be determined from the phase diagram. The particle transfer increases with increasing μ_L within a superfluid region and becomes constant as μ_L is moved into a Mott insulating zone where the system is incompressible. In the fermionization regime, the magnitude of Δn is fixed by Eq. (2). The analogous reasoning applies to the removal of particles at the battery pole with $\mu_R < \mu$.

Feeding atoms into a circuit element through a contact at one end and removing them through a contact at the other end generates a current. This current, after time averaging, reaches a constant value if the carrier excess at one end is replenished through one contact with the battery at the same rate at which the deficit is maintained at the other end through the contact with the other pole of the battery.

Experimentally, a battery can be created by establishing two separate large systems which act as reservoirs, each with its own constant chemical potential. These may also be lattices or other experimentally plausible systems, such as large harmonic traps, containing a large number of atoms. Changing the frequency of the harmonic traps, or adjusting the lattice height, can be used to tune the chemical poentials of these reservoirs. Each of these reservoirs can be connected to one end of the atomtronic system and current is then possible from the higher chemical potential system to the lower one. This configuration is displayed in Fig. 3. From a practical point of view, the chemical potentials of the battery poles can be maintained by transferring atoms, possibly classically, between the two poles.

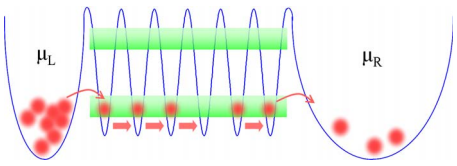

FIG. 3. (Color online) Schematic of atoms in a lattice connected to an atomtronic battery. A voltage is applied by connecting the system to two reservoirs, one of higher (left) and one of lower (right) chemical potential. An excess (deficit) of atoms is generated in the left (right) part of the system, giving rise to a current from left to right.

III. ATOMTRONIC CONDUCTORS

An attractive feature of atomtronic materials is that their conductivity properties can be easily modified. In this section, we first discuss the possibility of varying the conductivity of a material by lattice doping as is done in semiconductor systems. Second, we focus on the current-voltage characteristics of wires made of different types of atomtronic materials.

A. Doped materials

New materials with interesting properties can be designed by modifying the lattice in which the atoms are confined, and hence the many-body band structure. This can be done in various ways. In the case of an optical lattice, the periodicity of the lattice can be modified by superimposing a periodic potential of different wavelength [37]. Disorder can be introduced by randomly modifying individual sites [38–40]. A further handle on the properties of the material is the symmetry of a two-dimensional or three-dimensional lattice [41–43]. Finally, it is conceivable to introduce a second atomic species, either bosonic or fermionic, and to modify the properties of the material via interspecies interactions.

The atom analog of the doping of a semiconductor is particularly interesting. The aim of doping is to create energy levels in the energy gap between two bands. *N*-type doping is associated with energy levels located close to the lower edge of the first empty band while *P*-type doping gives rise to levels close to the upper edge of the highest full band. Both are accomplished by modifying the potential at individual lattice sites. *N*-type doping is achieved by replacing some lattice sites with donor sites. These correspond to potential wells which are slightly deeper than those of the unmodified lattice. Analogously, *P*-type doping requires introducing acceptor sites of slightly shallower potential. The two potential configurations are shown in Fig. 4.

The advantage of doping is that it can turn an insulator into a conductor without having to excite particles across the band gap into the empty conduction band. In atomtronics, this means that doping shifts the insulator zone boundary in the phase diagram. Figure 5 compares the phase diagram of the undoped lattice with that of a *N*-doped and a *P*-doped lattice. *N*-type doping shifts the insulating zone downwards such that states that were previously in the insulating zone come to lie right above the insulating zone where the lattice has a full valence band and a few free carriers in the conduction band. Similarly, *P*-type doping shifts the insulating zone upwards such that states previously in the insulating region come to lie right below the insulating zone where the lattice has an almost full valence band with a few free hole carriers. In Fig. 5 the new insulating zones were derived for an infinite lattice where every third site was doped by $\Delta\epsilon = \pm 5J$ using a modified Jordan-Wigner transformation [36]. The boundary between insulating and conducting zones were found in the same manner as discussed for the phase diagram of the uniform system in Sec. II A.

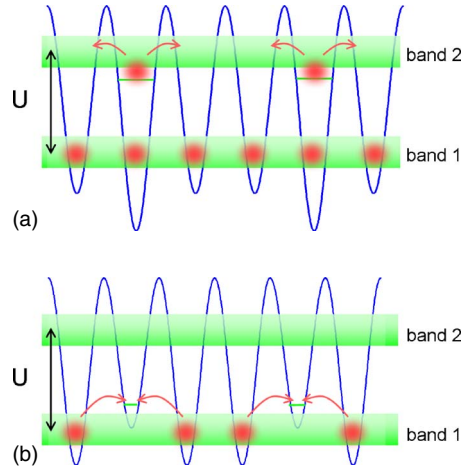

FIG. 4. (Color online) (a) Schematics of an *N*-doped lattice. The donor sites feature a level right below the first empty many-body band. An atom which occupies this level can easily be excited and move throughout the lattice. (b) Schematics of a *P*-doped lattice. Acceptor sites have a level right above the highest full band. Atoms can easily be excited into this level and allow for a hole to move throughout the lattice.

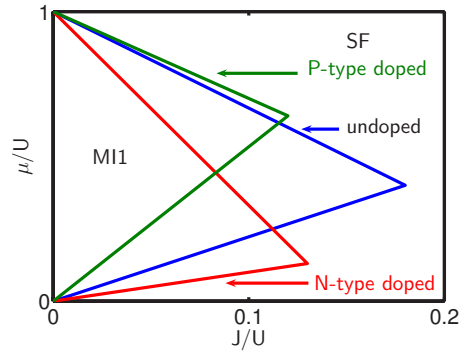

FIG. 5. (Color online) Zero temperature phase diagram of a Bose gas in an undoped (blue), an *N*-doped (red) and a *P*-doped (green) lattice. The boundary of the lowest Mott insulator lobe with a filling of one atom per site is displayed as calculated using the two-state approximation. The results for the doped lattices were obtained by adding an energy of $\pm 5J$ to every third site in an infinite lattice using a modified Jordan-Wigner transformation. *N*-type doping turns an insulating state into a superfluid state with more than one atom per site. Similarly, *P*-type doping turns an insulating state into a superfluid state with less than one atom per site.

B. Currents in atomtronic wires

This section discusses the current response of atomtronic wires to an applied voltage. The magnitude of the current depends on the properties of the material and on the nature of the contact with the battery. The material can be in the Mott insulating phase or in the superfluid phase. In the Mott phase, a small voltage does not yield a current. Only at a large voltage, of the order of the gap U, is the battery able to generate a current by feeding particles into the next unoccupied band. If the material is in the superfluid phase, a small voltage is enough to generate a current. Due to the superfluid nature of the atomic carriers, this current is not slowed by friction. Hence, the ratio of voltage to current does not have the physical meaning usually associated with resistance, but reflects the limits on the current at a given voltage due to factors other than dissipation. A primary limit is set by the hopping parameter J which quantifies how fast atoms can move from one site to the next. The value of the hopping parameter depends on the shape and the depth of the lattice. A further limit on the current is due to the interaction between atoms. Repulsion forces them to move in a highly correlated fashion. For this reason, the current does not grow linearly with the number of carriers at fixed voltage. Instead, the current per particle drops as more carriers are added and eventually goes to zero when the filling is one atom per site and the system becomes an insulator.

Apart from material dependent factors, the nature of the contact with the battery can set the maximum achievable current. If it is more difficult for atoms to pass through the contact than to hop from one lattice site to the next then the current is not limited by J but by the rate at which the battery can feed in and remove particles. This situation is encountered when operating a battery in a regime of very weak coupling. The same properties are present in electronic systems where there can be different types of contacts, such as rectifying and ohmic contacts [44]. In this paper we focus on the regime of maximum currents where currents are limited by the hopping parameter J and are not influenced by the properties of the battery contact (see the Appendix for details).

Figure 6 presents the current as a function of voltage for lattices, or wires, of average filling $n=1.1,1.3,1.5,1.7,1.9$. The calculation performed to obtain these current-voltage characteristic curves are described in the Appendix. At fixed filling, the current increases monotonically with increasing voltage. The maximum current attainable for a half-filled second band is $\sim 1.4J/\hbar$. The voltage in Fig. 6 is given in units of $\Delta\mu_{\max}$. This quantity denotes the chemical potential differences that yield the maximum currents. It corresponds to the chemical potential difference at which the system, for a given filling, enters an insulating regime at one of the two battery contacts.

The curves for fillings with an equal number of free particles and holes coincide, demonstrating the equivalence of hole and particle motion for $U \gg J$. The inset in Fig. 6 presents the currents at different average fillings, corresponding to different materials, at $\Delta\mu=\Delta\mu_{\max}$. The plot is symmetric around its maximum at half-filling reflecting particle-hole symmetry. Note that the average current per free particle, i.e., holes at $n>1/2$, is constant.

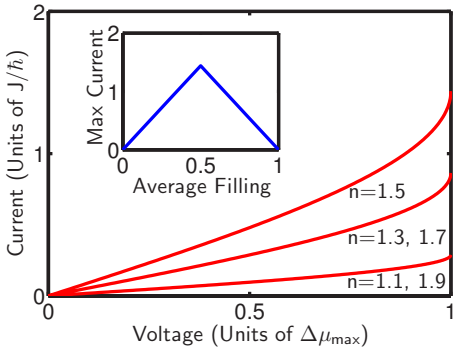

FIG. 6. (Color online) Current as a function of chemical potential difference (voltage) for different materials (different fillings n) in the fermionization regime where bosons are impenetrable. A wire with a certain number of atoms carries the same current as a wire with that number of holes (particle-hole symmetry). The chemical potential difference is given in units of $\Delta\mu_{\max}$. This quantity denotes the chemical potential differences that yield the maximum currents and corresponds to the chemical potential difference at which the system enters an insulating regime at one of the two battery contacts for a given n. Inset: Current as a function of filling at $\Delta\mu_{\max}$. Maximum currents are attained at half-filling. Note the symmetry in the current due to the particle-hole symmetry.

IV. ATOMTRONIC DIODES

A diode is a circuit element that features a highly asymmetric current-voltage curve. It allows a large current to pass in one direction, but not in the other. The analog of an electronic diode is an atomtronic circuit element that lets an atomic current pass through when applying a voltage $V=\mu_L-\mu_R$ while allowing no current or only a small saturation current for a voltage $V=-(\mu_L-\mu_R)$.

In solid state electronics, diodes are built by setting up a PN junction in which a P-type semiconductor is brought into contact with an N-type semiconductor. Electrons move through the junction until an equilibrium is reached. This process depletes the junction region of free charges, leaving behind the static charges of the donor and acceptor impurities. As illustrated in Fig. 7(a), this creates an effective potential step across the junction. When a reverse bias voltage is applied, the energy barrier is increased, reducing the flux of electrons from N-type to P-type. At the same time the number of electrons that can fall down the step remains constant giving rise to a reverse bias saturation current that is independent of voltage [see Fig. 7(b)]. However, if the diode is forward biased, more electrons are able to move from the N-type to the P-type material than at equilibrium since the potential barrier is decreased by the forward bias voltage [see Fig. 7(c)]. A detailed discussion of the diode behavior of a semiconductor PN-junction can, for example, be found in Ref. [44].

A. Diode *PN*-junction configuration

As discussed previously, we can design atomtronic wires whose conductivity properties can be described by locating the material's chemical potential in its phase diagram. Composite materials, such as PN-junctions, can be produced by

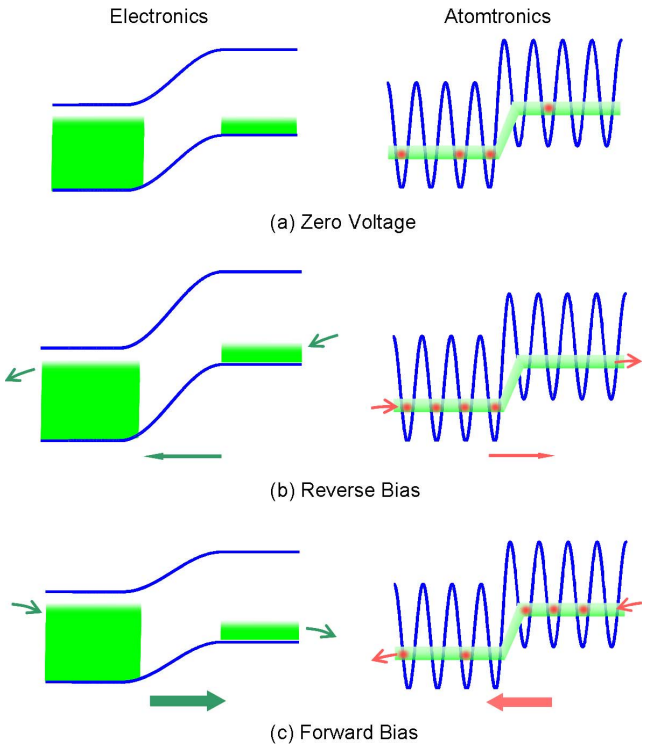

FIG. 7. (Color online) Schematic of the conduction band of an electronic (left-hand panels) and atomtronic (right-hand panels) *PN*-junction diode in (a) equilibrium, (b) reverse bias, and (c) forward bias with *N*-type materials on the left and *P*-type on the right of each configuration. Left-hand panels: The electronic system features a voltage dependent energy barrier at the junction leading to an increasing (decreasing) flux from the *N*-type to the *P*-type material as the junction is forward (reverse) biased while the current from *P* to *N* is independent of voltage. Right-hand panels: The operation of an atomtronic diode is based on the existence of insulating phases where $\partial n/\partial \mu = 0$, i.e., a change in voltage does not lead to a change in particle transfer between battery and system. As a consequence, only a small current can flow from *N*-component to *P*-component through an atomtronic diode in reverse bias while in forward bias the particle transfer between battery and system can be varied over a large range.

connecting lattices of different doping. Another possibility of building a junction is to superimpose additional external potentials, for example, a simple potential step. This has the effect of shifting the phase diagram of a part of the lattice upwards or downwards with respect to that of the rest. Since phase boundary effects are small, the state of the different components can be accurately described by the phase diagrams of the individual materials (see the Appendix for details). This means that a local chemical potential can be associated with each component of the conductor that can be located in each material's phase diagram. Thereby, the local conductivity properties can be identified. Of course, at equilibrium, i.e., at zero voltage, the composite material is actually described by a single chemical potential μ but it is μ relative to the zero point energy of each lattice site that determines the filling of each site.

In the following, we focus on a junction created by an external potential step since this may be the easiest experimental realization of a diode. The potential step could be generated experimentally by exposing one part of the system to off-resonant laser light. The main characteristics of the diode behavior are not affected by this choice.

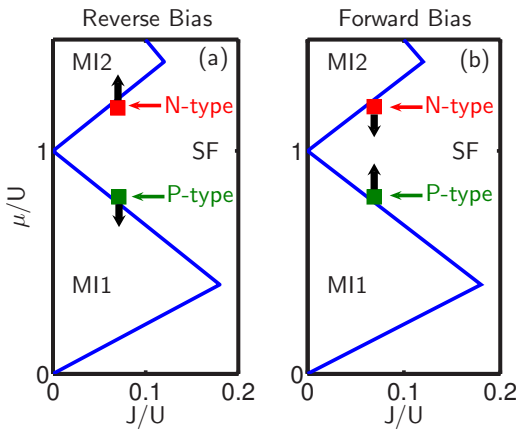

FIG. 8. (Color online) Phase diagram of the *PN*-junction configuration of an atomtronic diode. The small (large) population of the second many-body band in the *P*-type (*N*-type) material yields the analog of the small (large) thermal electron population of the conduction band in a semiconductor. The states of the *P*-type and *N*-type materials at zero voltage are represented by the squares. Arrows indicate the chemical potential difference (voltage) imposed to obtain a reverse (left) and a forward biased junction (right).

The conduction band of a semiconductor *PN*-junction features a small thermal electron population on the *P*-side and a considerably larger electron filling on the *N*-side. An example of an atomtronic equilibrium configuration with analogous features is represented by the squares in Fig. 8. The small (large) population of the second band in the *P*-type (*N*-type) material yields the analog of the small (large) thermal electron population of the conduction band in a semiconductor.

B. Diode current-voltage characteristics

To achieve diode characteristics, we exploit the possibility of undergoing a quantum phase transition between insulating and superfluid phases. The materials are configured such that the chemical potentials of the battery poles remain in the superfluid regime when hooking up the battery in one direction, but they easily enter insulating regimes when the voltage is applied in the opposite direction.

The effect of applying a voltage is illustrated in Fig. 8. Forward bias is achieved by connecting the *P*-side to the low voltage pole and the *N*-side to the high voltage pole of the battery. In this situation, the chemical potentials of the battery poles are located in the superfluid region of the phase diagram and atoms can flow from the *P*-component to the *N*-component. The larger the applied voltage, the larger the generated current. When the battery contacts are switched, the diode is reverse biased. As the voltage is increased a small current starts flowing. However, as soon as the voltage is large enough to make the battery chemical potentials enter the insulating zones, the current can not increase any further. As a consequence, the current-voltage curve is asymmetric.

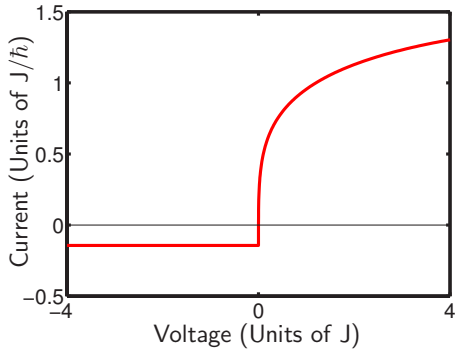

FIG. 9. (Color online) The characteristic current-voltage curve for an atomtronic diode. The larger the forward bias (voltage>0), the higher the current of atoms flowing from the *P*-component and to the *N*-component. In reverse bias (voltage<0) the current saturates since the particle transfer between battery and system cannot be increased beyond a certain small value when the battery pole chemical potentials enter insulating zones where $\partial n/\partial \mu = 0$.

The remnant current obtained in reverse bias, the saturation current, becomes smaller as the components' initial states are moved closer to the insulating phase.

Figure 7 presents a schematic comparison of the conduction band of an electronic and an atomtronic diode obtained using a step potential. For the atomtronic diode, the fact that only a small current can flow in reverse bias is not due to the presence of a voltage-dependent energy barrier at the junction as in the electronic case. Instead, it arises from the battery chemical potentials moving into insulating zones corresponding to a full conduction band on the *N*-side and an empty conduction band on the *P*-side. An important difference between electronic and atomtronic case is the opposite direction of current flow. In forward bias, atoms flow from the *P*-type to the *N*-type material as opposed to the other way around for electrons in a semiconductor.

Figure 9 displays the highly asymmetric current-voltage curve obtained from our calculation. The potential step is chosen such as to yield an equilibrium configuration with a filling of 1.99 and 1.01 atoms on the *N*-side and *P*-side respectively. In this configuration, we obtain a reverse saturation current of $0.14J/\hbar$ while in forward bias, currents can exceed $1.4J/\hbar$. Note that the current changes strongly in the vicinity of $V=0$. This is reminiscent of the behavior of an electronic diode as the temperature approaches zero. Reducing the potential step lowers the population difference between *P*-type and *N*-type materials at equilibrium and leads to an increase in saturation current and to a decrease in the slope of the current-voltage curve around $V=0$.

The diode currents have been calculated in the same manner as the currents carried by atomtronic wires except for the addition of the potential energy step between the two sites (see the Appendix for details of calculations).

V. ATOMTRONIC TRANSISTOR

As in electronics, the highly asymmetric current-voltage curve of atomtronic diodes can be exploited to build a transistor. Bipolar junction transistors (BJT) are circuit elements

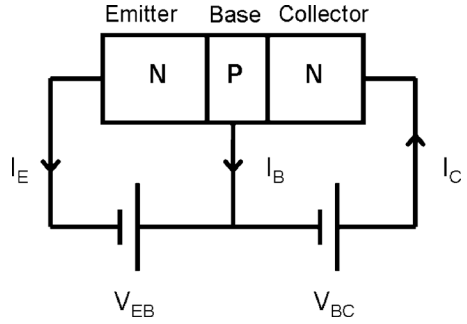

FIG. 10. Circuit schematic of an electronic or atomtronic bipolar junction transistor of the *NPN*-type. A thin *P*-type component (base) is sandwiched between two *N*-type components (emitter and collector). The key feature is that the voltage V_{EB} can be used to obtain gain in the collector current I_C relative to the base current I_B.

that can serve as amplifiers and switches. In electronics, they consist either of a thin *P*-type layer sandwiched between two *N*-type components (*NPN*) or a thin *N*-type layer between two *P*-type components (*PNP*). For our discussion, we consider a *PNP* configuration. A detailed discussion of semiconductor bipolar junction transistors can, for example, be found in Ref. [44]. The basic circuit schematic is displayed in Fig. 10. The voltage V_{BC} that is applied to the *PN*-junction formed by the middle component, the base, and one of the outer components, the collector, puts this junction into reverse bias. At the same time, the other junction formed by the base and the other outer component, the emitter, is put into forward bias by applying a voltage V_{EB}. The key idea is to use the voltage V_{EB} to control the current I_C leaving the collector element and thereby achieve differential gain in I_C relative to the base current I_B. At $V_{EB}=0$ one is simply dealing with the reverse biased base-collector junction. In this case, the currents I_C and I_B both equal the small reverse bias saturation current of the base-collector junction. The collector current I_C grows drastically when V_{EB} is increased such that the emitter-base junction is forward biased. This effect relies on the base region being very thin. The forward bias gives rise to a flow of electrons from the emitter into the base region, thereby significantly increasing the number of electrons at the base-collector junction. Recall that at $V_{EB}=0$, the base is depleted of electrons by the reverse bias V_{BC}. The emitter-base junction thus serves to greatly modify the number of carriers in the base that are subjected to the base-collector reverse bias. This leads to an increase of I_C beyond the saturation current. Since the base is extremely thin there is less opportunity for the electrons to leave the base compared to entering the collector. Because of this, most of the current that enters the base from the emitter moves on to the collector instead of it leaving out the base terminal. Therefore the relative changes in the current from the base I_B and from the collector I_C yields a large differential gain dI_C/dI_B.

These key features of an electronic transistor can be translated into atomtronics with atoms taking the place of electrons. The important point is to mimic the carrier densities and thus the fillings of the three components. This can be achieved by doping or, equivalently, by using potential steps. As with the diode, we focus on the latter implementation.

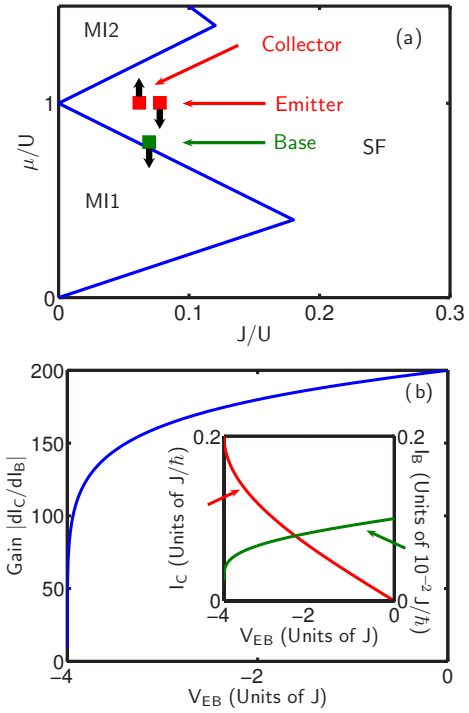

FIG. 11. (Color online) (a) Squares: equilibrium configuration of an atomtronic bipolar junction transistor in the phase diagram. Arrows: direction in which the chemical potentials of the battery contacts are varied. (b) Differential gain dI_C/dI_B as a function of emitter-base voltage V_{EB}. Inset: Base current and collector current as a function of emitter base voltage. The voltage is changed by varying the emitter contact potential from $\mu(n_E=1)$ to $\mu(n_E=1.5)$. The base contact is kept at $\mu(n_B=1)$ right below its equilibrium value $\mu(n_B=1.005)$ while the collector contact is kept at the equilibrium value $\mu(n_C=1.5)$.

The atomtronic transistor can be created by setting up a configuration such that for zero voltage the conduction bands of the left-hand and right-hand regions have a large filling compared to the sandwiched thin base region. The phase diagram for such an arrangement is depicted in Fig. 11(a), where the squares represent the equilibrium configuration, while the arrows indicate the way the battery chemical potentials are tuned. A small voltage is applied to the collector-base junction such that a small current flows from the collector into the base. When the emitter battery chemical potential μ_E is lowered, atoms move from base to emitter and leave through the emitter, giving rise to a nonzero emitter current I_E. As a back-effect, this leads to an increase in I_C since the fast removal of atoms from the base through the emitter allows more atoms to move into the base from the collector. Meanwhile, the base current I_B becomes smaller the further the emitter chemical potential μ_E is lowered. This is due to the base being very thin relative to the emitter and the collector, so atoms traverse preferentially from collector to emitter rather than leaving out the base, thereby contributing to I_B. The effect of the forward bias V_{EB} on the base current I_B is thus opposite to its effect on I_C. Therefore, our atomtronic transistor features an inverted amplification in which a small decrease in the base current goes along with a large increase in the collector current (negative gain).

An example for the behavior of the currents in an atomtronic transistor is given in Fig. 11(b). The equilibrium configuration has 1.5 atoms per site in emitter and collector and 1.005 atoms per site in the base. In Fig. 11(b) we plot data obtained for the individual currents I_C and I_B upon variation of the emitter chemical potential μ_E while keeping the base battery contact at a chemical potential $\mu(n_B=1)$ in the $n=1$ Mott-insulating zone and the collector contact at $\mu(n_C=1.5)$. To demonstrate differential gain we display the quantity $|dI_C/dI_B|$ as a function of V_{EB}. The details of the calculation are presented in the Appendix.

VI. REMARKS

We have shown how strongly interacting ultracold bosonic gases in periodic potentials can be used as conductors and insulators in a circuit and how they can be employed to build atomtronic analogs of diodes and bipolar junction transistors. From here, the implementation of an atom amplifier is immediate. An atom amplifier is a device that allows control of a big atomic current with a small one. The transistor presented above directly serves this purpose since small changes in the base current bring along large changes in the collector current. It is straightforward to conceive of more complex devices such as a flip flop, a bistable device that uses cross negative feedback between two transistors.

The similarity in qualitative behavior goes along with a number of significant differences in the underlying physics. First, in the atomic case the energy gap results from interactions rather than from statistics as in electronics. Second, the atomic currents are superfluid. As a consequence, the ratio between voltage and current has the meaning of a dissipationless resistance. Further differences arise in both diodes and transistors. Our atomtronic diode does not feature a depletion layer, i.e., it does not exhibit a voltage-dependent energy barrier at the junction. The asymmetry in the current-voltage curve results from voltage-sign dependent quantum phase transitions to an insulating phase. As a consequence, atoms flow from *P*-type to *N*-type in forward bias rather than flowing, as in electronics, from *N*-type to *P*-type. Note that this difference cannot be resolved by drawing the analogy between atom holes and electrons rather than atoms and electrons since this would also require relabeling the *N*-type material as *P*-type and vice versa and hence the current direction would again be reversed in comparison to the electronic case. Due to the difference in diode behavior the atomic collector current in a transistor flows from collector into base and the emitter current flows from base into emitter, i.e., opposite to electronic flow in a *NPN* transistor. A significant difference in the qualitative behavior of electronic and atomtronic transistor is given by the gain being negative in the atomtronic case. The collector current increases as the base current decreases. We expect that this does not affect the functionality of devices based on the operation of bipolar junction transistors. Yet, an adaptation of their design will be necessary.

The data presented in this paper is obtained from calculations for a one-dimensional lattice. This choice is of an entirely practical nature. The basic ideas also hold for two- and

three-dimensional cubic lattices and extend to other lattice geometries that make transitions between superfluid and insulating phases upon changes of the chemical potential.

Working with higher-dimensional lattices increases the magnitude of the currents that can be achieved. In an one-dimensional optical lattice with an experimentally realizable depth of $10E_R$ the hopping parameter $J \sim 0.02E_R$, where $E_R = \hbar^2\pi^2/2md^2$ is the recoil energy which is fixed by the lattice period d. For 87 Rb and a lattice period of $d=400$ nm, the recoil energy is $E_R=(2\pi\hbar)3.55$ kHz yielding currents on the scale $J/\hbar \sim 2\pi \times 71$ Hz. This implies, that the currents through a three-dimensional lattice of the same period and depth with a cross-section of 10×10 sites are of the order $(100\times 2\pi)\times 71$ Hz.

Experiments aimed at atomtronic devices will be challenging given the current status of ultracold atom technology. Among other challenges is the need to combine atomic potentials that have typically been demonstrated in isolated systems, and, moreover, is the need to spatially cascade regions in which atoms undergo nonlinear interactions. An optical lattice might well serve as the basis for fabricating atomtronic *P*-type and *N*-type materials. Alternatively, lattice potentials could be created by passing current through microfabricated wires on the chip surface. And perhaps coupling an atom magnetic waveguide to an optical or nonoptical lattice as a means of transporting atoms to and from the lattice can set the stage for atom diode experiments. In principle, atom chips provide the means for supporting different types of atomic potentials on a single substrate. The lattice systems used in atomtronic circuits do not necessarily have to support coherent currents. The important feature is that the system's tendency to accept or not accept particle transfer from the battery exhibits the incompressibility associated with the Mott insulating phase. We have provided a conceptual framework of semiconductor material and device analogs that can serve as building blocks to more sophisticated atomtronic devices and circuits. An in-depth discussion of actual atomtronic device implementation necessarily goes beyond the scope of this work.

An issue to be addressed in the future is that of the noise associated with the inherent quantum uncertainty of the current carrying states given the context, at least on some length scales, of the coherent transport of atoms.

Finally, it is important to keep in mind that this paper develops atomtronics within the Bose-Hubbard model. This model provides an excellent description of ongoing experiments with ultracold bosonic atoms in optical lattices. Other Hamiltonians might offer alternative ways of drawing the analogy with electronics. A natural choice for further study are Hamiltonians describing bosons with beyond onsite interactions and Hamiltonians for fermionic gases.

ACKNOWLEDGMENTS

The authors thank John Cooper, Rajiv Bhat, and Brandon M. Peden for useful discussions. This work was supported by the Defense Advanced Research Projects Agency's Defense Science Office through a PINS program (Grant No. W911NF-04-1-0043) and the Air Force Office of Scientific Research (Grant No. FA9550-04-1-0460). The authors also acknowledge support of the Department of Energy, Office of Basic Energy Sciences via the Chemical Sciences, Geosciences, and Biosciences Division, furthermore of the National Science Foundation (B.T.S.) and the Deutsche Forschungsgemeinschaft (M.K.).

APPENDIX: CALCULATIONAL DETAILS

In the following, we discuss the calculation of the current-voltage characteristics presented in Figs. 6, 9, and 11. The role of the system size is considered in Sec. A 1. The results of this discussion justify the use of small systems in the calculation of the current response to a given voltage. Our approach is developed in Secs. A 1–A 4. These three sections discuss the effect of the battery on the system, the character of the resulting current carrying state and the way these two aspects are used as a starting point in formulating our method to calculate the current-voltage characteristics. The details of the algorithm used for wires and diodes are laid out in Sec. A 5. Finally, the calculation for the transistor is discussed in Sec. A 6.

1. Small system considerations

There are three primary concerns about the system size when performing calculations with a small lattice: effects on the phase diagram, effects at the boundary between two phases and effects on the current. All of these effects we find to be small.

Although phase diagrams of ultracold bosons in lattices, strictly speaking, refer to infinite systems, it is possible to describe phase diagrams for much smaller systems in a similar manner. For example, phase diagrams can be created for systems that are only four or six sites large. For a small system, the Mott insulator phase can be defined as a state with an integer filling of the lattice. The superfluid phase is defined by a state with noninteger filling of the lattice. Note that adding an extra atom to a small system does require slightly more energy than adding an extra atom to an infinite system because in a large system the atom can distribute itself among more sites than for a small system. This, however, does not appreciably affect the characteristics of the different phases. The phase diagrams for small systems are similar to that presented for an infinite system in Fig. 2. The tip of the lobe is moved only slightly and the width of the superfluid region, where the lattice has noninteger filling and number fluctuations are large, only changes from $2J$ for a system of only two sites to $4J$ for an infinite lattice. The width of the superfluid region is already $1.6J$ for six sites. In addition, the number fluctuations characteristic of superfluid and insulating phase do not depend on the system size and only vary on the order of a few percent between small and large systems of the same filling. Similarly, the doped phase diagrams presented in Fig. 5 do not change considerably when calculated for small systems. The phase diagrams of these systems all possess the same qualitative feature that the insulating zone of the *N*-type doped lattice is pushed downwards while the insulating zone of the *P*-type doped lattice is

pushed upwards. In conclusion, we find that small systems can be used to replicate the infinite lattice relations $\mu(n)$ plotted in Figs. 2 and 5.

Adjoining *P*-type and *N*-type materials creates a junction at which boundary effects could alter each component. However, we have found that the boundary only minimally affects one to two sites of each component in the limit $U \gg J$. We have examined the ground state of a *PN* configuration that extends over 20 lattice sites and compared each side with *P*-type and *N*-type materials in the absence of a junction. The difference in the occupation numbers and their fluctuations between the two systems is on the order of a few percent for the first site at the junction and is down to a tenth of a percent by the third site. In conclusion, using the expression $\mu(n)$ of *P*-type and *N*-type materials to describe each side of a *PN*-junction individually in a small system is justified because boundary effects due to the interface between the two materials are small.

Finally, the third reason why small systems can be used to model larger systems is that the net current is not significantly affected by the size of the system. We have verified this numerically by comparing the exact dynamical evolution in one-dimensional lattices of between two and 10 sites at constant filling with periodic boundary conditions. In the initial state, the density is modulated with period $2d$ and there is a constant phase difference between neighboring sites. This initial state is an example of the kind of running wave that would be created by a battery (as will be discussed below). The evolution of this state with the Hamiltonian Eq. (1) within the two-state approximation yields a net current that does not significantly depend on the number of lattice sites. This property is reminiscent of the current carried by a Bloch state which is independent of the system size at fixed quasimomentum. A good estimate of the current response can therefore be obtained by considering a very small number of links. In this way, it is possible to circumvent calculating the dynamics of a large lattice. Note that even within the two-state approximation such a dynamical calculation is feasible only for systems with a small number of sites.

2. Battery contacts

To power a circuit, the system is connected to an atomtronic battery by bringing two reservoirs of different chemical potential μ_L and μ_R into contact with the two ends of the lattice. The values of μ_L and μ_R determine the particle transfer Δn which is injected through one contact and removed through the other. The transfer Δn follows from the relations $\mu_L(n+\Delta n)$ and $\mu_R(n-\Delta n)$ with n the filling of the system at zero voltage. Note that the chemical potentials μ_L and μ_R should be chosen appropriately to ensure that the average filling is kept at n.

The net current obtained by applying a voltage is given by the average number of particles passing through the system per unit time after a transient time has passed. The net current not only depends on the particle transfer Δn as determined by the values of μ, μ_L, and μ_R, but also on the strength of the coupling between battery and system. The latter is set by the properties of the battery contact and determines the rate at which transfers of magnitude Δn take place.

3. Maximum current solution

The maximum current is obtained when subsequent transfers of the battery are separated by the time it takes for one transfer of Δn to free up the site to which the battery is connected. Such a situation is achieved for transfer rates that are close to $J/\hbar$. This is the regime we focus on. It yields the largest currents and reveals the limits on the currents that are due to the properties of the material rather than due to the properties of the battery contact.

The state reached after a time of transient behavior takes the form of a running density wave. The maxima (minima) of the wave take the value $n+\Delta n$ ($n-\Delta n$) and, hence, the wave amplitude depends on the voltage. The wavelength is given by twice the lattice period at maximum current. Note that in the limit of small voltages, the wave created by the contact with the battery can be described by the elementary excitations of the gas.

4. Current response calculation

The computation of the full dynamics of a realistic system would require a simulation of a large lattice interacting with several reservoirs, one at each battery contact. Instead, we use a simplified small-system approach. This approach does not allow us to describe the transient behavior. We expect the duration of the transient to be set by the time it takes for the particle transfer Δn from the battery to traverse the $(M-1)$ links of a lattice with M sites. Hence, the transient should occur on the time scale of $(M-1)(\hbar/J)$.

Our calculation of the current response is performed in two steps: First, the particle transfer Δn at a given voltage is determined from the relation $\mu_L(n+\Delta n)$ [or, equivalently, from $\mu_R(n-\Delta n)$] for an infinite lattice with the help of Eq. (2). Second, using the results of the first section, we calculate the net current in a small system carried by a running wave with amplitude Δn and wavelength $2d$, where d is the lattice period. This requires preparing an initial state that corresponds to the momentary state of such a wave and to evolve it in time yielding a time-dependent current. The net current is given by the average particle transfer per unit time.

5. Atomtronic wires and diodes

As discussed above in Sec. A 1, currents can be calculated by considering small systems. As a consequence, for a simple atomtronic wire the second step of the calculation, i.e., the calculation of the net current carried by a wave of amplitude Δn and wavelength $2d$, can be carried out by considering a single link.

In an atomtronic diode, it is the interface region rather than the bulk *P*-type or *N*-type material that poses the biggest obstacle for atom flow and thus determines the net current. The current calculation can be reduced down to just this single interface link since the evolution is little affected by adding further surrounding sites.

For a given transfer from the battery Δn, the current response of a single link is calculated using an initial state with $n_R=n+\Delta n$ particles on the right and $n_L=n-\Delta n$ particles on the left. The initial phase relation between the two sites is chosen so as to produce the lowest energy configuration that has the given filling on each site. We then compute the dynamical evolution yielding the time-dependent current $i(t)$. The net current I is obtained by calculating the time average of $i(t)$ over the time interval Δt and maximizing it with respect to Δt. With ν the frequency of the density oscillation, the time it takes for $2\Delta n$ particles to move from the initially higher populated site to its neighbor is given by $1/2\nu$. Hence, the result for the net current is approximately given by $I=4\Delta n\nu$.

To calculate the currents through an atomtronic wire (see Sec. III, in particular Fig. 6) we consider a single link in the absence of additional external potentials with an equilibrium occupation $1<n<2$. The evolution of the two site system yields the time-dependent current

$$i(t)=\frac{2J}{\hbar}(n_R-n_L)\sin(4Jt/\hbar). \tag{A1}$$

To obtain the net current we maximize the time average of Eq. (A1) over a time interval Δt. This yields

$$I=1.45\frac{J}{\hbar}(n_R-n_L) \tag{A2}$$

with $\Delta t=0.58\hbar/J$. This result is close to the value $I=4\Delta n\nu$ with the Rabi frequency $\nu=2J/\hbar\pi$. From the result for the relation $I(\Delta n)$ we obtain the current-voltage dependence $I(\Delta\mu)$ using Eq. (2) for an infinite lattice.

The current characteristics of a diode (see Sec. IV) is calculated in the same way with a potential step included between the two lattice sites. This potential step ensures that the two sides have the desired difference in occupation at equilibrium. In this configuration, the calculation yields a slightly more complicated current relation.

6. Transistor

The calculation for the transistor are performed in a similar way as that for a wire or a diode. Similar to the case of the diode, the current response to particle transfer from the battery is determined by the atom flux through the two interfaces between emitter-base and base-collector. Moreover, as discussed earlier, the current response has a small dependence on the number of links. Therefore, the current can be calculated by considering a three-site system, the two links representing the two links at the two interfaces of the *NPN* system. An external potential is added to raise the middle site playing the role of the base while the outer sites represent the emitter and collector.

The initial state is prepared as the lowest energy state with a variable number of n_E atoms in the emitter and $n_C=1.5$ atoms in the collector. The filling on the base is determined from the height of the potential on the base and the condition of being in the lowest energy state with fillings n_E and n_C on the emitter and collector. At equilibrium ($n_C=n_E=1.5$), the base is occupied by $n_B=1.005$ atoms. The current of atoms passing through the base from collector to emitter is given by $i_C=(i_{CB}+i_{BE})/2$ with i_{CB} the current from collector to base and i_{BE} the current from base to emitter. As in the preceding sections, we calculate the net collector current I_C by maximizing the time average of i_C. Since we are interested in the μ_E dependence of I_C at fixed V_{BC}, the initial collector occupation is kept fixed at $n_C=1.5$ while the emitter occupation n_E is varied in the range $1\leqslant n_E<1.5$.

The base current is set to be $I_B=\Gamma(n_B-1)$, where Γ must satisfy the condition $\Gamma\ll J/\hbar$. The quantity Γ describes the weak coupling with the battery at the base contact which is due to the thinness of the base. The data for I_B displayed in Fig. 11(b) is obtained using $\Gamma=0.01J/\hbar$. The number of current carriers involved in I_B is given by (n_B-1) because the chemical potential of the base contact is set to be in the $n=1$ insulator region. Note that our calculation neglects the effect of I_B on I_C. This is justified because the weak coupling at the base contact implies that the reduction of n_B by I_B is small. Overall, the transistor current gain relies on two factors. The base region must be thin and the emitter must have an equilibrium filling significantly larger than the base.

[1] B. P. Anderson and M. A. Kasevich, Science **282**, 1686 (1998).

[2] F. Cataliotti, S. Burger, C. Fort, P. Maddaloni, F. Minardi, A. Trombettoni, A. Smerzi, and M. Inguscio, Science **293**, 843 (2001).

[3] M. Greiner, I. Bloch, O. Mandel, T. W. Hänsch, and T. Esslinger, Phys. Rev. Lett. **87**, 160405 (2001).

[4] O. Morsch, J. H. Müller, M. Cristiani, D. Ciampini, and E. Arimondo, Phys. Rev. Lett. **87**, 140402 (2001).

[5] J. Denschlag, J. Simsarian, H. Häffner, C. McKenzie, A. Browaeys, D. Cho, K. Helmerson, S. Rolston, and W. Phillips, J. Phys. B **35**, 3095 (2002).

[6] G. Modugno, F. Ferlaino, R. Heidemann, G. Roati, and M. Inguscio, Phys. Rev. A **68**, 011601(R) (2003).

[7] G. Roati, E. de Mirandes, F. Ferlaino, H. Ott, G. Modugno, and M. Inguscio, Phys. Rev. Lett. **92**, 230402 (2004).

[8] L. Pezze, L. Pitaevskii, A. Smerzi, S. Stringari, G. Modugno, E. De Mirandes, F. Ferlaino, H. Ott, G. Roati, and M. Inguscio, Phys. Rev. Lett. **93**, 120401 (2004).

[9] C. Fort, F. Cataliotti, J. Catani, L. De Sarlo, L. Fallani, J. Lye, M. Modugno, R. Saers, and M. Inguscio, Laser Phys. **15**, 447 (2005).

[10] M. Köhl, H. Moritz, T. Stöferle, K. Günter, and T. Esslinger, Phys. Rev. Lett. **94**, 080403 (2005).

[11] D. Jaksch, C. Bruder, J. I. Cirac, C. W. Gardiner, and P. Zoller, Phys. Rev. Lett. **81**, 3108 (1998).

[12] M. Greiner, O. Mandel, T. Esslinger, T. W. Hänsch, and I. Bloch, Nature (London) **415**, 39 (2002).

[13] T. Stöferle, H. Moritz, C. Schori, M. Köhl, and T. Esslinger, Phys. Rev. Lett. **92**, 130403 (2004).
[14] A. Ruschhaupt and J. G. Muga, Phys. Rev. A **70**, 061604(R) (2004).
[15] A. Micheli, A. J. Daley, D. Jaksch, and P. Zoller, Phys. Rev. Lett. **93**, 140408 (2004).
[16] A. Ruschhaupt, F. Delgado, and J. G. Muga, J. Phys. B **38**, 2665 (2005).
[17] A. Ruschhaupt and J. G. Muga, Phys. Rev. A **73**, 013608 (2006).
[18] A. Ruschhaupt, J. G. Muga, and M. G. Raizen, J. Phys. B **39**, L133 (2006).
[19] A. J. Daley, S. R. Clark, D. Jaksch, and P. Zoller, Phys. Rev. A **72**, 043618 (2005).
[20] A. Micheli and P. Zoller, Phys. Rev. A **73**, 043613 (2006).
[21] J. Stickney, D. Z. Anderson, and A. Zozulya, Phys. Rev. A **75**, 013608 (2007).
[22] S. Rolston and W. Phillips, Nature (London) **416**, 219 (2002).
[23] K. Bongs and K. Sengstock, Rep. Prog. Phys. **67**, 907 (2004).
[24] C. Search and P. Meystre, in *Progress in Optics*, edited by E. Wolf (Elsevier, Amsterdam, 2005), Vol. 47.
[25] G. K. Brennen, C. M. Caves, P. S. Jessen, and I. H. Deutsch, Phys. Rev. Lett. **82**, 1060 (1999).
[26] H. Briegel, T. Calarco, D. Jaksch, J. Cirac, and P. Zoller, J. Mod. Opt. **47**, 415 (2000).
[27] A. Steane, Rep. Prog. Phys. **61**, 117 (1998).
[28] R. Folman, P. Krüger, J. Schmiedmayer, J. Denschlag, and C. Henkel, Adv. At., Mol., Opt. Phys. **48**, 263 (2002).
[29] J. Reichel, Appl. Phys. B: Lasers Opt. **75**, 469 (2002).
[30] W. Zwerger, J. Opt. B: Quantum Semiclassical Opt. **5**, S9 (2003).
[31] M. P. A. Fisher, P. B. Weichman, G. Grinstein, and D. S. Fisher, Phys. Rev. B **40**, 546 (1989).
[32] P. Jordan and E. Wigner, Z. Phys. **47**, 631 (1928).
[33] S. Sachdev, *Quantum Phase Transitions* (Cambridge University Press, Cambridge, 1999).
[34] R. Bhat, L. D. Carr, and M. J. Holland, Phys. Rev. Lett. **96**, 060405 (2006).
[35] The lower and/or upper boundary of the mth Mott zone is obtained by applying the two-state approximation to the mth/$(m+1)$th many-body band, where $m=1,2,\ldots$ is the many-body band index. The tip of the zone, given by the intersection of the two boundaries, yields a good estimate of the value of J/U at which the superfluid-insulator transition occurs at integer filling.
[36] B. M. Peden (unpublished).
[37] S. Peil, J. V. Porto, B. Laburthe Tolra, J. M. Obrecht, B. E. King, M. Subbotin, S. L. Rolston, and W. D. Phillips, Phys. Rev. A **67**, 051603(R) (2003).
[38] P. Horak, J.-Y. Courtois, and G. Grynberg, Phys. Rev. A **58**, 3953 (1998).
[39] H. Gimperlein, S. Wessel, J. Schmiedmayer, and L. Santos, Phys. Rev. Lett. **95**, 170401 (2005).
[40] T. Schulte, S. Drenkelforth, J. Kruse, W. Ertmer, J. Arlt, K. Sacha, J. Zakrzewski, and M. Lewenstein, Phys. Rev. Lett. **95**, 170411 (2005).
[41] L. Santos, M. A. Baranov, J. I. Cirac, H. U. Everts, H. Fehrmann, and M. Lewenstein, Phys. Rev. Lett. **93**, 030601 (2004).
[42] L. Sanchez-Palencia and L. Santos, Phys. Rev. A **72**, 053607 (2005).
[43] G. Grynberg and C. Robilliard, Phys. Rep. **355**, 335 (2001).
[44] P. D. Ankrum, *Semiconductor Electronics* (Prentice-Hall, Englewood Cliffs, NJ, 1971).